ESTABLISHMENT AND VALIDATION OF A THEORETICAL MODEL FOR SINGLE LONGITUDINAL AXIAL FLOW THRESHING AND SEPARATION OF MILLET
/
谷子单纵轴流脱粒分离理论模型的建立与验证

Jun-hui ZHANG[1)], Lin ZHAO[2)], Shu-juan YI[*1)], Dong-ming ZHANG[1)], Xin ZHANG[3)]
[1)]College of Engineering, Heilongjiang Bayi Agricultural University, Daqing/P.R.China
[2)]Beijing Polytechnic, Beijing, 100176, China
[3)]Engineering Technology Research Institute, Daqing Drilling Engineering Co., Ltd., Daqing 163319, China
Tel: +86-459-13836961877; E-mail: yishujuan_2005@126.com
Corresponding author: Shu-juan YI
DOI: https://doi.org/10.35633/inmateh-76-09

Keywords: *millet, cumulative threshing rate, cumulative separation rate, fitting, test*

ABSTRACT
The influence of the device's structure and operating parameters, along with the material properties of millet, on threshing and separation performance forms the theoretical basis for designing and researching a single longitudinal axial flow threshing and separation device specifically adapted to millet. Therefore, a theoretical model for grain threshing and separation in a single longitudinal axial flow threshing device was established based on variable mass theory. To validate the theoretical model, single-factor tests were conducted on the feeding rate, rotational speed, and water content of Longgu 31 millet. The error analysis between the experimental and calculated values indicates that within a moisture content range of 17.14% to 32.93%, feeding rates varying from 1 to 3 kg/s, and rotational speeds ranging from 700 to 1000 r/min, the R-squared values consistently exceed 0.97. This indicates an excellent fit of the theoretical model. The theoretical model will serve as a valuable reference for the design and investigation of the single longitudinal axial flow separation device.

摘要
谷子的物料特性和装置的结构参数、工作参数对脱分性能的影响，是适应谷子特性的单纵轴流脱分装置设计和研究的理论依据。因此，应用变质量理论建立了谷子在单纵轴流脱分装置内的脱分理论模型，并构造了脱粒参数和分离参数的表达式。为了验证理论模型，选取龙谷 31 号为试验对象，在搭建的单纵轴流脱粒分离试验台上开展了谷子的喂入量、转速、含水率单因素试验，并将试验数据与模型计算数据进行误差分析，对比结果表明：当含水量为 17.14%-32.93%、喂入量为 1-3kg/s，转速为 700-1000r/min 时，试验数据与模型计算数据的 R-Squared 误差均大于 0.97，理论模型的拟合度好。因此，理论模型将为单纵轴流脱离分离装置的设计和研究提供参考。

INTRODUCTION
Currently, the grain combine harvester has become an indispensable agricultural machine for field operations. As a critical component, the threshing device plays a pivotal role in determining the overall performance of the harvester. Consequently, numerous scholars have devoted significant effort to optimizing this essential mechanism.

The tangential flow threshing device was utilized in early harvesting machinery, and its theoretical model has been well-established. The effects of structural design, operational parameters, and material properties on the threshing and separation efficiencies of the tangential flow threshing device were elucidated (*Wan et al., 1990; Zhang et al., 1994*). Due to its longer threshing time and superior threshing and Separation performance, the axial-flow threshing and Separation device has become predominantly used in grain combine harvesters in recent years. Consequently, scholars have conducted extensive theoretical and experimental research on the threshing and Separation performance of axial-flow devices. The authors investigated the effects of structural and operational parameters of the axial flow threshing device on threshing rate and separation rate through experimental research, and subsequently optimized these parameters (*Liu et al., 2021;*

Jun-hui Zhang, Ph.D.; Lin Zhao, Ph.D.; Shu-juan Yi, Prof. Ph.D.; Dong-ming Zhang, Ph.D.; Xin Zhang, master degree

Wu et al., 2022; Zhang et al., 2025; Liu et al., 2023). Through theoretical analysis, a separation probability model for the vertical axial flow threshing and separation device was developed. The results demonstrate that the structural and motion parameters of the drum significantly influence separation efficiency (*Dong et al., 1988*). In recent years, with millet and other coarse grain crops are more and more recognized by the public, millet harvesting process mechanization requirements are higher and higher. Research on the mechanical properties of millet grains and stems has progressively deepened, providing a solid foundation for the development of threshing devices specifically adapted to the unique characteristics of millet (*Zhang et al., 2018; Zhang et al., 2019; Yang et al., 2015*). Through experimental studies on the threshing process of millet, it was concluded that the rasp bar type axial flow method is most suitable for threshing and separating millet due to its specific characteristics (*Liang et al., 2015; Kang et al., 2017*).

In conclusion, while extensive experimental research has been conducted on the longitudinal axial flow threshing and separation process, there is a notable deficiency in the literature regarding theoretical models of this process. It is imperative to elucidate the impact of grain material characteristics, structural parameters, and operational parameters of the threshing device on the performance of the longitudinal axial flow threshing and separating system. This research will provide a theoretical foundation for designing and developing a longitudinal axial flow threshing and separating device tailored to the specific characteristics of millet.

MATERIALS AND METHODS

Structure and working principles of the single longitudinal axial flow threshing and separation device

The single longitudinal axial flow threshing and separation device is shown in Fig. 1(a). This device primarily comprises the feeding mechanism, threshing cylinder, cover plate, material collection trolley, and control system.

When the device is working, millet is fed into the axial threshing and separation device through the feeding device, and the action process of grain in the single longitudinal axial flow threshing and separation device can be divided into two distinct phases: threshing and separation. The threshing process is completed by rubbing and striking between the rasp bar-nail teeth combined threshing components, the concave plate and the material in the drum. The threshed seeds overcome the resistance of the stalk layer, pass through the grid of the concave plate, and fall into the material collection trolley, thereby completing the separation process.

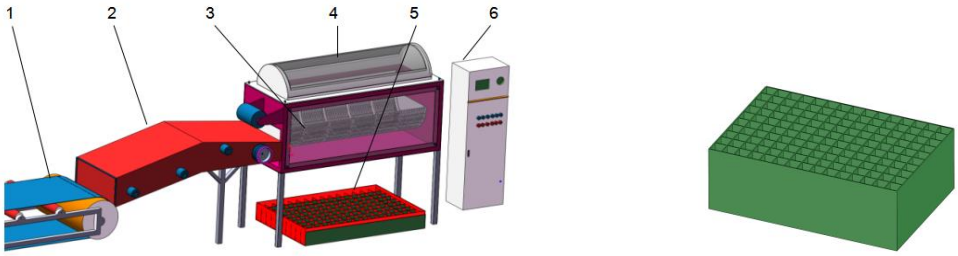

(a) Primarily comprises of the device *(b) Material collection trolley*

Fig. 1 - Diagram illustrating the single longitudinal axial flow threshing and separation device

1 – Conveyor; 2 – Feeding mechanism; 3 – Threshing cylinder; 4 – Cover plate; 5 – Material collection trolley; 6 – Control system

The material collection trolley (as showed in Fig. 1(b)) consists of a 14×16 matrix of collection buckets, with each bucket measuring 10cm×10cm. During the single longitudinal axial flow threshing and separation device test, this trolley is employed to gather materials threshed from different locations within the device.

Theoretical model for the single longitudinal axial flow threshing and separation device

The cumulative separation rate is a critical metric for evaluating the performance of the axial flow threshing and separation device. This parameter is influenced by the physical properties of the grain, as well as the structural and operational parameters of the threshing and separation device. In the process of investigating their relationship, the following assumptions were made to streamline the calculations.

① The probability of grain being threshed and separated in the single longitudinal axial flow threshing and Separation device varies along the axial position. This variation is influenced by the characteristic parameters of the grain as well as the structural and operational parameters of the device.

② The probability of grains being threshed within an axial differential element is directly proportional to the quantity of unthreshed grains within that infinitesimal segment.

③ The likelihood of threshed grains being separated is directly proportional to the quantity of threshed but unseparated grains contained within the differential elements.

The coordinate system (as show in Fig. 2) was established on the single longitudinal axial flow threshing and separation device.

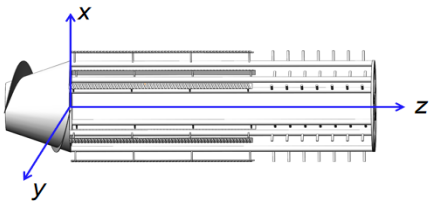

Fig. 2- The coordinate system of the single longitudinal flow threshing and separation device

(1) Threshing and separation model of the rasp bar section

The length of the rasp bar section was expressed as z_1 (as shown in Fig. 3). The total grain mass per unit length in the single longitudinal axial flow threshing and separation device was set as unit 1. The ratio of grain to grass was denoted by γ. And the cumulative threshing rate at the distance z from the feeding inlet was set as *T(z)*. When $0 \le z \le z_1$, the axial micro segment was located in the rasp bar part of the combined threshing and separation component. According to the second assumption, the cumulative threshing rate increment *dT* in differential element *dz* can be expressed as follows.

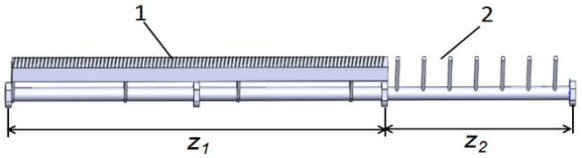

Fig. 3 - The configuration of the rasp bar-nail tooth threshing element
1 – Rasp bar section; 2 – Nail tooth section

$$dT(z) = a_{11}\frac{\gamma}{1+\gamma}\big(1 - T(z)\big)dz \tag{1}$$

where a_{11} is the threshing parameter of the rasp bar section. It is related to the characteristic parameters of millet, the structural parameters and working parameters of the single longitudinal axial flow threshing and separation device.

According to the actual working situation, the cumulative threshing rate of millet is zero when z equals zero. That is $T(z)|_{z=0} = 0$. By applying the method of separation of variables and integrating the differential equation in Equation (1), the cumulative threshing rate was obtained as follows:

$$T(z) = 1 - exp\left(-\frac{a_{11}\gamma}{1+\gamma}z\right) \tag{2}$$

The cumulative separation rate at the distance z from the feeding inlet was set as $F(z)$. According to the third assumption, the cumulative separation rate increment dF in axial differential element dz can be expressed as follows:

$$dF(z) = a_{12}\frac{\gamma}{1+\gamma}\big(T(z) - F(z)\big)dz \tag{3}$$

where a_{12} is the separation parameter of the rasp bar section.

According to the actual working situation, the cumulative separation rate of millet is zero when z equals zero. That is $F(z)|_{z=0} = 0$. Substituting this into Equation (3), the following expression is obtained:

$$F(z) = 1 + \frac{a_{12}}{a_{11} - a_{12}}exp\left(-\frac{a_{11}\gamma}{1+\gamma}z\right) - \frac{a_{11}}{a_{11} - a_{12}}exp\left(-\frac{a_{12}\gamma}{1+\gamma}z\right) \tag{4}$$

It can be seen from Equation (2) and (4) that both the cumulative threshing rate and the cumulative separation rate of the rasp bar section are an exponential function of the axial coordinate z.

(2) Threshing and separation model of the nail tooth section

The length of the nail tooth section was expressed as z_2 (as shown in Fig. 3). When $z_1 \le z \le z_1+z_2$, the axial micro-segment was located in the nail tooth section of the combined threshing and separation component. According to the second assumption, the cumulative threshing rate increment *dT* in differential element dz can be expressed as follows.

$$dT(z) = a_{21}\frac{\gamma}{1+\gamma}\big(1 - T(z)\big)dz \tag{5}$$

where a_{21} is the threshing parameter of the nail tooth section.

According to Equation (2), when $z = z_1$, the cumulative threshing rate can be determined and subsequently integrated into Equation (5). Then, by applying the method of separation of variables, the cumulative threshing rate of the nail tooth section can be obtained.

$$T(z) = 1 - exp\left(-\frac{a_{21}\gamma}{1+\gamma}z - \left(\frac{a_{11}\gamma}{1+\gamma} - \frac{a_{21}\gamma}{1+\gamma}\right)z_1\right) \tag{6}$$

According to the third assumption, the cumulative separation rate increment dF in axial differential element dz can be expressed as follows:

$$dF(z) = \frac{a_{22}\gamma}{1+\gamma}\big(T(z) - F(z)\big)dz \tag{7}$$

where a_{22} is the separation parameter of the nail tooth section.

From Equation (4), it can be seen that when $z = z_1$, the cumulative separation rate can be determined and then the expression for the cumulative separation rate can be derived as follows:

$$\begin{aligned} F(z) = 1 + \frac{a_{22}}{a_{21}-a_{22}}exp\left(-\frac{a_{21}\gamma}{1+\gamma}(z-z_1) - \frac{a_{11}\gamma}{1+\gamma}z_1\right) \\ + \left(F(z_1) - 1 - \frac{a_{22}}{a_{21}-a_{22}}exp\left(-\frac{a_{11}\gamma}{1+\gamma}z_1\right)\right)exp\left(-\frac{a_{22}\gamma}{1+\gamma}(z-z_1)\right) \end{aligned} \tag{8}$$

It can be seen from Equations (6) and (8) that both the cumulative threshing rate and the cumulative separation rate of the nail tooth section are an exponential function of the axial coordinate z.

Construction of the threshing parameters and the separation parameters

From the derivation of the cumulative threshing rate $T(z)$ and the cumulative separation rate $F(z)$, it is evident that both the threshing parameters a_{11}, a_{21} and the separation parameters a_{12}, a_{22} are dimensionless quantities. In order to determine the threshing parameters and the separation parameters, the threshing process and the separation process of the single longitudinal axial flow threshing and separation device were analyzed.

(1) Construction of the threshing parameters

In the threshing and separation space, there is a periodic impact and rubbing between the rasp bar-nail tooth threshing element and the grain material through the high speed rotation of the threshing component. The grain will be separated from main stem when the acting force between the rasp bar threshing element and the grain material exceeds the connection force of grain and petiole, petiole and branch, branch and main stem. Then the threshing process of the grain will be completed (as Figure 4a).

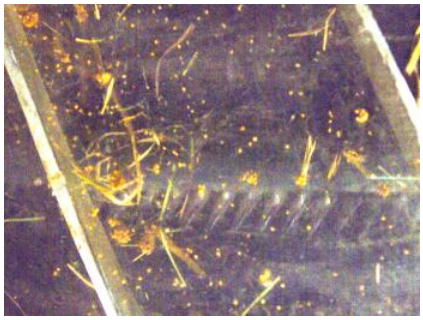

(a) Threshing process of the grain

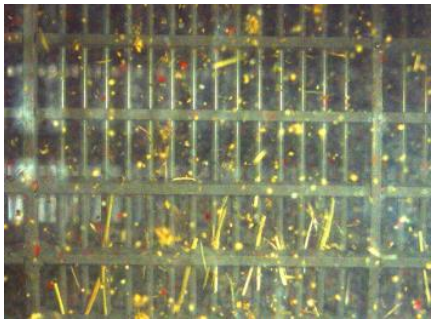

(b) Separation process of the grain

Fig. 4 - Threshing and separation process of the grain

The interaction force between the rasp bar section and grain material is mainly determined by the number of rasp bars, the number of transverse lattice on the concave plate and the relative linear velocity between rasps bar and grain material. The connection force of grain and petiole, petiole and branch, branch and main stem is related to the moisture content of millet. According to the analysis of the influencing factors in the threshing process and the theory of dimensional analysis, the following expression of the threshing parameter a_{11} was constructed.

$$a_{11} = c_{10} + c_{11}\frac{n_1 n_2}{h} + c_{12}\frac{n_1 n_2}{hv} \tag{9}$$

where n_1 is the number of rasp bar, n_2 is the number of concave panels, v is the linear velocity of the bar, h is the moisture content of grain, c_{10}, c_{11} and c_{2} are undetermined coefficients.

The interaction force between the nail tooth section and grain material mainly depends on the number of nail teeth, the diameter of nail teeth, the distance between nail teeth and the relative linear speed of the material. According to the theory of dimensional analysis, the following expression of the threshing parameter a_{21} was constructed.

$$a_{21} = c_{20} + c_{21}\frac{n_0 n_1 d_0}{l_0 h} + c_{22}\frac{n_0 n_1 d_0}{l_0 h v} \tag{10}$$

where n_0 is the number of nail teeth in a single combined threshing component, d_0 is the diameter of the nail teeth, l_0 is the distance between nail teeth, c_{20}, c_{21} and c_{22} are undetermined coefficients.

(2) Construction of the separation parameters

The threshed grains need to pass through the stem layer in the single longitudinal axial flow threshing and separation device and then through the grid gap of the concave plate to complete the separation process (as shown in Figure 4b). The resistance of grains passing through the stem layer is proportional to the thickness of the stem layer *(Yi et al., 2008; Vlăduţ et al., 2022)*. The thickness of the stem layer in the threshing separation space mainly depends on the size of the threshing and separation device, the feeding rate of millet, the density of grains and the movement time of grains in the threshing separation space. Therefore, it is assumed that the probability of the grain passing through the stalk layer is inversely proportional to the resistance of the stalk layer. And the resistance of the straw layer is directly proportional to the feeding rate and it is inversely proportional to the roller radius, rotational speed and grain density. The larger the area of grid holes in the concave plate, the easier it is for the seeds to separate through the concave plate. Therefore, it is assumed that the probability of the grain passing through the concave plate is directly proportional to the area of the grid hole of the concave plate. According to the theory of dimensional analysis, the following parameter expressions are constructed.

$$a_{12} = c_{10} + c_{11}\frac{\rho(2R - n_2 l_1)(l - n_3 d_1)}{q} + c_{12}\frac{\rho(2R - n_2 l_1)(l - n_3 d_1)v}{q} \tag{11}$$

where ρ is the density of the grain, n_3 is the number of concave strips, d_1 is the diameter of a concave strip, l_0 is the length of threshing drum, l_1 is the width of the transverse lattice of the concave plate, q is the feed rate, C_{10}, C_{11} and C_{12} are undetermined coefficients.

In the nail tooth section, the stirring effect of nail teeth makes the material in the threshing space loose and increases the probability of grains passing through the stem layer and being separated from the concave plate gap. The separation parameter of the nail teeth is also influenced by the number of nail teeth, their height and the distance between them. According to the theory of dimensional analysis, the following parameter equation is constructed.

$$a_{22} = C_{20} + C_{21}\frac{\rho n_0 n_1 h_0(2R - n_2 l_1)(l - n_3 d_1)}{l_0 q} + C_{22}\frac{\rho n_0 n_1 h_0(2R - n_2 l_1)(l - n_3 d_1)v}{l_0 q} \tag{12}$$

where h_0 is the height of nail teeth, C_{20}, C_{21} and C_{22} are undetermined coefficients.

Fitting test and validation test

Longgu 31 was selected as the test material to carry out the single longitudinal axial flow threshing and separation test in the harvest laboratory of Heilongjiang Bayi Agricultural University (as shown in Fig. 5). The ratio of grain to grass was 1.61. The grain density was 1053 kg/m^3.

(1) Fitting test

There were undetermined coefficients in the threshing parameters a_{11}, a_{21} and the separation parameters a_{12}, a_{22} of the single longitudinal axial flow threshing and separation theoretical model. In order to determine these undetermined coefficients, a single longitudinal axial flow threshing and separation device was built and laboratory tests were carried out. Then the undetermined coefficients in the theoretical model could be determined by fitting equation (4) and (8) with the test data.

The feeding rate was 1.5kg/s. And the grain moisture content was 25% ± 1%. The rotational speed was 800 r/min. All the experiments were repeated 3 times.

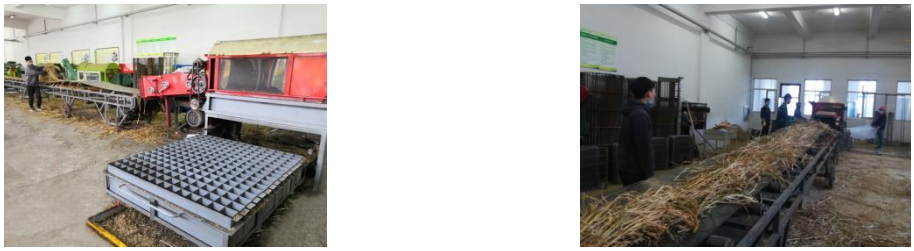

(a) Experiment preparation *(b) Experiment in progress*

Fig. 5 - Laboratory testing of threshing and separation performance for Millet

(2) Validation test

To validate the theoretical model, single-factor experiments were conducted on moisture content, feeding rate, and rotational speed. The moisture content of millet was varied between 17% and 32%. The feeding rate was set within the range of 1.5 kg/s to 3.0 kg/s. The rotational speed was tested in the range of 600 to 1000 r/min.

The material receiving trolley was used to collect threshed material from different axial coordinates. The millet in each bucket was separated, weighed, and the weight recorded. At the same time, the mixed millet and unthreshed millet were collected at the straw outlet, weighed, and the weight recorded. Formula (13) was applied to calculate the separation rate of the receiving bucket numbered *i*, and formula (14) was used to calculate the cumulative separation rate at coordinate *z*.

$$F_i = \frac{m_i}{\sum_{i=1}^{14} m_i + m_{mixed} + m_{unthreshed}} \times 100\% \quad (13)$$

$$F(z_i) = \frac{\sum_{j=1}^{i} m_j}{\sum_{i=1}^{14} m_i + m_{mixed} + m_{unthreshed}} \times 100\% \quad (14)$$

RESULTS

The fitting results of undetermined coefficients for threshing parameters and separation parameters

The variation data of the cumulative separation rate along the axis, obtained under the aforementioned test conditions, were presented in Table 1.

Table 1

Single longitudinal axial flow threshing separation laboratory test data of millet

z	Cumulative separation rate			
	Test one	Test two	Test three	Mean value
[m]	[%]	[%]	[%]	[%]
0.00	0.0000	0.0000	0.0000	0.0000
0.01	7.0721	6.8296	6.2932	6.7316
0.02	19.9198	17.7207	18.9419	18.8608
0.03	37.7734	35.6278	41.6141	38.3384
0.04	50.2412	51.9599	56.1289	52.7767
0.05	66.9131	66.4892	71.4036	68.2686

z	Cumulative separation rate			
	Test one	Test two	Test three	Mean value
[m]	[%]	[%]	[%]	[%]
0.06	78.1907	78.2470	80.8602	79.0993
0.07	84.7583	85.2418	86.6465	85.5489
0.08	88.9557	88.4965	90.2538	89.2353
0.09	91.7402	92.3759	93.5216	92.5459
0.10	94.1897	94.7856	95.4434	94.8062
0.11	96.3431	96.6883	97.1033	96.7115
0.12	98.0653	97.6089	98.1360	97.9368
0.13	99.0231	98.5088	98.7495	98.7605
0.14	99.6204	99.3768	99.3977	99.4650

Curve fitted in MATLAB was utilized to fit the data. The fitted process was divided into two segments: the rasp bar section and the nail tooth section, as the cumulative separation rate was a piecewise function. For $0 \le z \le z_1$, the cumulative separation rate of the rasp bar section was fitted using the test data. Consequently, the values of the undetermined coefficients in the threshing and separation parameters were obtained. The equations of a_{11} and a_{12} were then determined as follows:

$$a_{11} = -2.918 + 0.02976\frac{n_1 n_2}{h} - 0.4989\frac{n_1 n_2}{hv} \tag{15}$$

$$a_{12} = 3.867 + 0.01523\frac{\rho(2R - n_2 l_1)(l_0 - n_3 d_1)}{q} + (8.031e - 05)\frac{\rho(2R - n_2 l_1)(l_0 - n_3 d_1)v}{q} \tag{16}$$

Based on the established threshing parameter a_{11} and separation parameter a_{12} in the rasp bar section, parameter fitting for the nail tooth section was carried out. Consequently, the undetermined coefficients a_{21} and a_{22} were obtained. The equations for a_{21} and a_{22} were then determined as follows:

$$a_{21} = 8.165 - 2.464\frac{n_0 n_1 d_0}{l_0 h} + 4.999\frac{n_0 n_1 d_0}{l_0 hv} \tag{17}$$

$$a_{22} = -3.662 + 0.02495\frac{\rho n_0 n_1 h_0(2R - n_2 l_1)(l - n_3 d_1)}{l_0 q} + (5.037e - 04)\frac{\rho n_0 n_1 h_0(2R - n_2 l_1)(l - n_3 d_1)v}{l_0 q} \tag{18}$$

Error Analysis of Calculated Values and Validation Experiments

To validate the accuracy of the theoretical model, a single-factor experiment of millet was conducted using the single longitudinal axial flow threshing and separation device. The factors selected for testing included millet moisture content, feeding rate, and rotational speed. For each varying factor, the separation rate within the buckets was measured, and cumulative separation rate curves as functions of the axial coordinate were plotted. These experimental curves were subsequently compared with the fitted curve obtained from the theoretical model.

(1) Evaluation of the fitting effect of moisture content as a single factor

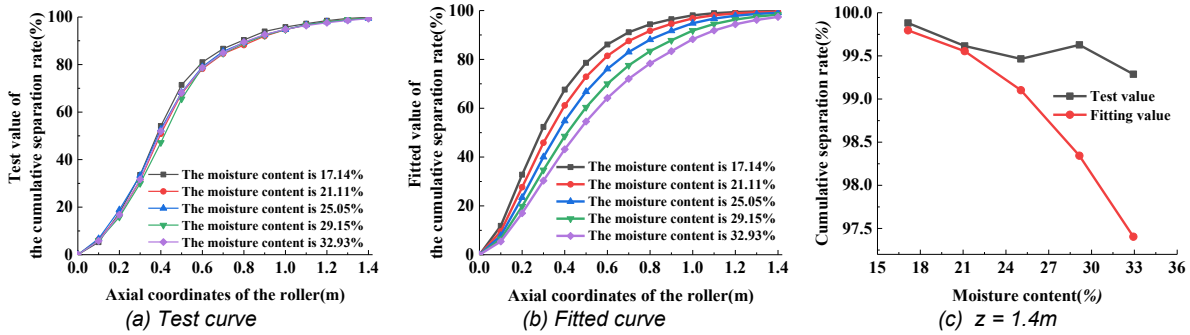

(a) Test curve (b) Fitted curve (c) z = 1.4m

Fig. 6 - Cumulative separation rate curve under varying moisture content conditions

Table 2

Error analysis table for single factor test of moisture content

	Error	Moisture content [%]				
		17.14	21.11	25.05	29.15	32.93
Rasp bar section	SSE	0.0926	0.0514	0.0049	0.0245	0.0848
	R-Squared	0.9769	0.9863	0.9987	0.9934	0.9777
Nail tooth section	SSE	0.0015	0.0014	0.0001	0.0039	0.0169
	R-Squared	0.9997	0.9997	0.9999	0.9993	0.9969
Rasp bar-Nail tooth	SSE	0.0934	0.0522	0.0049	0.0264	0.0931
	R-Squared	0.9893	0.9938	0.9994	0.9968	0.9890

The rotational speed was set to 800 r/min, the feeding rate was maintained at 2 kg/s, and the moisture content levels of the millet samples were 17.14%, 21.11%, 25.05%, 29.15%, and 32.93%. The experimental results and fitted values of the cumulative separation rate under different moisture contents were illustrated in Fig. 6. Table 2 presents the SSE and R-Squared values for both the fitted and tested data, specifically detailing the errors for the rasp bar section, the nail tooth section, and the combined rasp bar-nail tooth configuration.

As shown in Fig. 6a) and b), the experimental and fitted values of the cumulative separation rate exhibit exponential distributions with the axial coordinates. On the same axial coordinate, as water content increases, the magnitude of change in the fitting value exceeds that of the test value. As illustrated in Fig. 6c), upon completion of the threshing separation process, both the experimental and fitted values of the cumulative separation rate exceed 97%. As the moisture content increases, both the measured cumulative separation rate and the fitted cumulative separation rate exhibit a downward trend. However, the magnitude of change differs: the measured value decreases by 0.6%, while the fitted value decreases by 2.39%. As shown in Table 2, the SSE values for the rasp bar section, nail tooth section, and the combination of rasp bar - nail tooth components are all less than 1, while the *R-squared* values exceed 0.97. This indicates that the established threshing separation model fits well with changes in moisture content. However, the *R-squared* values for the rasp bar section are consistently lower than those for the nail tooth section, indicating that the model fits the rasp bar section less accurately compared to the nail tooth section.

(2) Evaluation of the fitting effect of feeding rate as a single factor

When the moisture content of millet was 25.0±0.2% and the rotational speed was set to 800 r/min, a single-factor experiment on feeding rate was conducted using the single longitudinal axial flow threshing and separation device. The feeding rate tested were 1.5 kg/s, 2.0 kg/s, 2.5 kg/s, 3.0 kg/s, and 3.5 kg/s. Fig. 7 presents the tested and fitted values of the cumulative separation rate under these different feeding quantities. Table 3 presents the *SSE* and *R-Squared* values for both the fitted data and test data in the single-factor experiment concerning feeding rate.

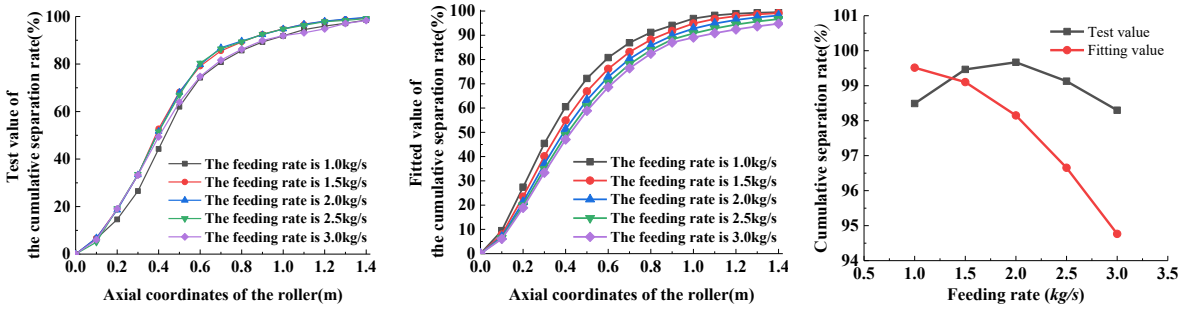

(a) Test curve *(b) Fitted curve* *(c) z = 1.4m*

Fig. 7 - Cumulative separation rate curve under varying feeding rate conditions

Table 3

Error analysis table for single factor test of feeding rate

	Error	Feeding rate [kg/s]				
		1.0	1.5	2.0	2.5	3.0
Rasp bar section	SSE	0.1031	0.0049	0.0157	0.0266	0.0120
	R-Squared	0.9704	0.9987	0.9960	0.9931	0.9966

	Error	Feeding rate [kg/s]				
		1.0	1.5	2.0	2.5	3.0
Nail tooth section	SSE	0.0076	0.0001	0.0022	0.0071	0.0052
	R-Squared	0.9986	0.9999	0.9996	0.9987	0.9990
Rasp bar-Nail tooth	SSE	0.1084	0.0049	0.0172	0.0319	0.0163
	R-Squared	0.9862	0.9994	0.9980	0.9963	0.9980

As shown in Fig. 7a) and b), the experimental and fitted values of the cumulative separation rate exhibit exponential distributions with the axial coordinates. As illustrated in Fig. 7c), upon completion of the threshing separation process, the measured cumulative separation rate exceeded 98.30%. The lowest fitted value was 94.76% at a feeding rate of 3.0 kg/s, resulting in a discrepancy of -3.54% between the fitted and measured values. As shown in Table 3, the *R-Squared* values for both the nail tooth section and the rasp bar-nail tooth combination element exceed 0.98. The minimum R-Squared value for the rasp bar section is 0.97, with all fitting values exceeding 0.95. The aforementioned results indicate that the function model exhibits satisfactory fitting performance in response to variations in feeding rate. However, the fitting accuracy for the rasp bar is comparatively lower than that for the nail tooth.

(3) Evaluation of the fitting effect of rotational speed as a single factor

When the moisture content of millet was 25.0 ± 0.20% and the feeding rate was 2.5 kg/s, a single-factor experiment on rotational speed was conducted using the single longitudinal axial flow threshing and separation device. The tested rotational speeds included 600 r/min, 700 r/min, 800 r/min, 900 r/min, and 1000 r/min. Fig. 8 shows the measured and fitted values of cumulative separation efficiency under different rotational speeds. Table 4 shows the *SSE* and *R-Squared* values for both the fitted and test datasets in the single-factor experiment related to rotational speed.

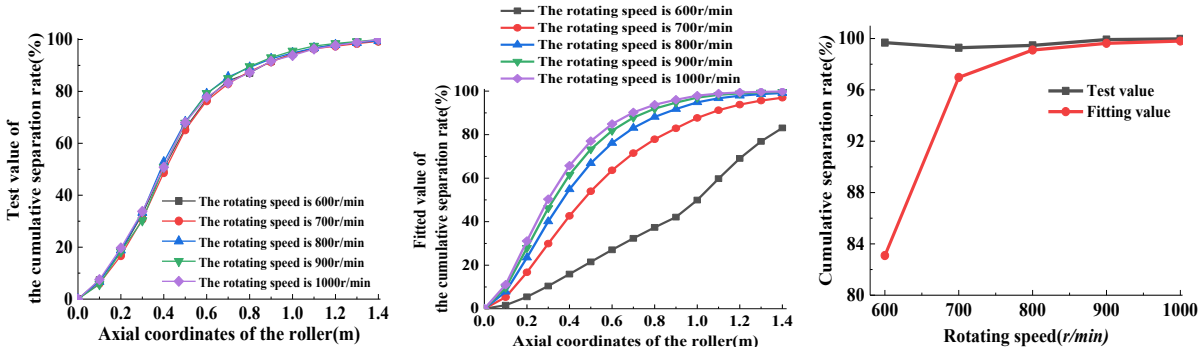

(a) Test curve (b) Fitted curve (c)z = 1.4m

Fig. 8 - Cumulative separation rate curve under varying rotational speed conditions

Table4

Error analysis table for single factor test of rotational speed

	Error	Rotational speed [r/min]				
		600	700	800	900	1000
Rasp bar section	SSE	1.3940	0.0624	0.0049	0.0534	0.0884
	R-Squared	0.6211	0.9827	0.9987	0.9860	0.9763
Nail tooth section	SSE	0.7390	0.0168	0.0001	0.0006	0.0046
	R-Squared	0.8653	0.9969	0.9999	0.9999	0.9992
Rasp bar-Nail tooth	SSE	1.8879	0.0722	0.0049	0.0537	0.0911
	R-Squared	0.7741	0.9913	0.9994	0.9937	0.9891

It can be observed from Fig. 8a) and Fig. 8b) that at the rotational speed of 600 r/min, the fitted curve significantly deviates from the test curve. Furthermore, as shown in Fig. 8(c), when the rotational speed is 600 r/min and z = 1.4, the fitted cumulative separation rate is 83.09%, resulting in a difference of -16.59% compared to the test value. As illustrated in Table 4, when the rotating speed is 600 r/min, the *SSE* values for the rasp bar section and the rasp bar-nail tooth combination exceed 1.

Additionally, the *R-Squared* values for the rasp bar, nail tooth, and rasp bar-nail tooth combination are 0.62, 0.86, and 0.77, all of which are significantly lower than the threshold of 0.95. Consequently, the function model exhibits poor fitting performance at this rotating speed. When the speed is set to 700 r/min, 800 r/min, 900 r/min, and 1000 r/min, the *SSE* values are all below 0.1, while the *R-Squared* values exceed 0.97. Therefore, the function model demonstrates excellent fitting performance.

CONCLUSIONS

(1) Based on the material characteristics of millet, a threshing and separation model utilizing a single longitudinal axial flow threshing separation device was developed. Analysis revealed that both the cumulative threshing rate and the cumulative separation rate of the rasp bar section and the nail tooth section exhibited exponential relationships with the axial coordinate. By examining the threshing and separation processes of millet within the single longitudinal axial flow threshing and separation device, functional expressions for the threshing parameters and separation parameters were formulated.

(2) A single longitudinal axial flow threshing and separation test platform was developed to perform fitting tests. The undetermined coefficients of the threshing and separation parameters were determined through data fitting using Matlab. This process clarified the influence of structural and material parameters on both the cumulative threshing rate and cumulative separation rate of the single longitudinal axial flow threshing and separation device.

(3) A single-factor test was conducted using the longitudinal axial flow threshing and separation device. Through the error analysis of the single-factor test curve and the fitting curve, it was found that when the moisture content ranged from 17.14% to 32.93%, the feed rate was between 1 and 3 kg/s, and the rotational speed was within 700-1000 r/min, the R-Squared values for both the calculated and experimental cumulative separation rate function models exceeded 0.97. This indicates that the model exhibits excellent fit and theoretical capability.

REFERENCES

[1] Dong, C., & Jiang, Y. (1988). Experimental Investigation of the Grain Separation Mechanism and Improvement of Separation Performance in Vertical Axial Flow Separation, Rethreshing, and Cleaning Integrated Devices (籽粒分离机理和提高立置轴流分离、复脱、清选三合一装置分离性能的试验研究) [J]. *Journal of Agricultural Mechanization Research*, (02), 6-16. China.

[2] Kang, D., Wu, C., Liang, S., & Tang, Q. (2017). Design and Test of The Threshing Device of Millet Combine Harvester (谷子联合收获机脱粒装置设计与试验)[J]. *Journal of China Agricultural University*, *22*(02), 135-143. China.

[3] Liang, S., Jin, C., Zhang, F., Kang, D., & Hu, M. (2015). Design and Experiment of 4LZG-3.0 Millet Combine Harvester (4LZG-3.0 型谷子联合收获机的设计与试验) [J]. *Transactions of the Chinese Society of Agricultural Engineering*, *31*(12), 31-38. China.

[4] Liu, J., Wang, D., He, X., Shang, S., Xu, N., Guo, P., Yin, S., & Yang, X. (2021). Design and Experiment of Threshing Device of Sesame Combine Harvester (芝麻联合收获机脱粒装置的设计与试验) [J]. *Journal of Agricultural Mechanization Research*, *12*, 110-114. China.

[5] Liu, W., Ma, L., Zong, W., Liu, J., Li, M., & Lian, G. (2023). Design and Experimentation of a Longitudinal Axial Flow Sunflower Oil Threshing Device [J]. *Agriculture*, *Switzerland, 13*(4), 876. https://doi.org/10.3390/agriculture13040876

[6] Vlăduţ N-V., Biriş S-Ş., Cârdei P., Găgeanu I., Cujbescu D., Ungureanu N., Popa L-D., Perişoară L., Matei G., Teliban G-C. (2022). Contributions to the Mathematical Modeling of the Threshing and Separation Process in an Axial Flow Combine [J]. *Agriculture*, *12*(10), 1520. https://doi.org/10.3390/agriculture12101520

[7] Wan, J., Zhao, X., & Ji, C. (1990). A Mathematical Model for Conventional Grain Thresher and its Application (传统型脱粒装置的数学模型及应用) [J]. *Transactions of the Chinese Society of Agricultural Machinery,* (2), 49-56. China.

[8] Wu, J., Tang, Q., Mu, S., Jiang, L., & Hu, Z. (2022). Test and Optimization of Oilseed Rape (Brassica napus L.) Threshing Device Based on DEM[J]. *Agriculture*, *Switzerland, 12*(10), 1580. https://doi.org/10.3390/agriculture12101580

[9] Yang, Z., Sun, J., & Guo, Y. (2015). Effect of Moisture Content on Compression Mechanical Properties and Frictional Characteristics of Millet Grain (不同含水率对谷子籽粒压缩力学性质与摩擦特性的影响) [J]. *Transactions of the Chinese Society of Agricultural Engineering*, *31*(23), 253-260. China.

[10] Yi, S., Wang, C. Mao, X., & Tao, G. (2008). Observation and Analysis of Motion Rule of Free Kernel in Threshing and Separating Space (轴流滚筒脱粒后自由籽粒空间运动规律的观察与分析) [J]. *Transactions of the Chinese Society of Agricultural Engineering,* (5), 136-139. China.

[11] Zhang, F., & Pang, Q. (2025). Optimization Design of Threshing Device for Dual Longitudinal Flow Combine Harvester (双纵轴流联合收割机脱粒装置优化设计) [J]. *Tractor and Farm Transporter*, *52*(1), 56-60. China.

[12] Zhang, J., & Du, L. (1994). Theoretical Study of Mathematical Model on Threshing and Separating Process (脱粒部件数学模型的建立与模拟)[J]. *Transactions of the Chinese Society of Agricultural Machinery*, (25), 56-60. China.

[13] Zhang, Y., Cui, Q., & Li, H. (2018). Effects of Stem Region, Moisture Content and Blade Oblique Angle on Mechanical Cutting of Millet Stem [J]. *INMATEH-Agricultural Engineering*, *55*(2), 105-112.

[14] Zhang, Y., Cui, Q., & Lin, X. (2019). Variations and Correlations of Shearing Force and Feed Nutritional Characteristics of Millet Straw (谷子秸秆剪切力与其饲料营养特性变化规律及相互关系) [J]. *Transactions of the Chinese Society of Agricultural Engineering*, *35*(5), 41-50. China.